1990

An Experimental Evaluation of the Heat Transfer Coefficients of R-134a Relative to R-12

M. W. Spatz
Allied-Signal Inc.

Jing Zheng
Allied-Signal Inc.

AN EXPERIMENTAL COMPARISON OF EVAPORATION AND CONDENSATION HEAT TRANSFER COEFFICIENTS FOR HFC-134a AND CFC-12*

S. J. Eckels   M. B. Pate
Department of Mechanical Engineering
Iowa State University
Ames, Iowa 50011

ABSTRACT

Experimental heat transfer coefficients are reported for HFC-134a and CFC-12 during in-tube single-phase flow, evaporation, and condensation. These heat transfer coefficients were measured in a horizontal, smooth tube with an inner diameter of 8.0 mm and a length of 3.67 m. The refrigerant in the test tube was heated or cooled by using water flowing through an annulus surrounding the tube. Evaporation tests were performed for a refrigerant temperature range of 5 to 15°C with inlet and exit qualities of 10% and 90%, respectively. For condensation tests, the refrigerant temperature ranged from 30 to 50°C, with inlet and exit qualities of 90% and 10%, respectively. The mass flux was varied from 125 to 400 $\frac{kg}{m^2 s}$ for all tests. For similar mass fluxes, the evaporation and condensation heat transfer coefficients for HFC-134a were significantly higher than those of CFC-12. Specifically, HFC-134a showed a 35 to 45% increase over CFC-12 for evaporation and a 25 to 35% increase over CFC-12 for condensation. A more representative comparison of the heat transfer coefficients for HFC-134a and CFC-12 is based on flow rates closer to those found in actual systems. Comparing HFC-134a and CFC-12 in refrigeration cycles with similar cooling capacities shows that HFC-134a has a lower mass flow rate in the evaporator and condenser because the enthalpy of vaporization is higher. At similar cooling capacities for an evaporator, the heat transfer coefficients for HFC-134a are 5 to 15% higher than CFC-12 while at similar heating capacities for a condenser they are 10 to 20% higher.

NOMENCLATURE

A	= area
C	= specific heat
h	= convective heat transfer coefficient
LMTD	= log mean temperature difference
m	= mass flow rate
Q	= heat transfer rate
T	= temperature
U	= overall heat transfer coefficient

Subscripts

i	= inner tube
in	= inlet
o	= annulus
out	= outlet
R	= refrigerant
sat	= saturation
T	= test section

INTRODUCTION

Experimental heat transfer evaluations of HFC-134a and other alternative refrigerants have become increasingly important as reductions in CFC's take effect. Since the thermodynamic properties of the two refrigerants are similar, HFC-134a is considered a potential replacement for CFC-12. HFC-134a is also more environmentally acceptable because of its zero ozone-depletion factor.

*An extended version will be published in the November, 1990 issue of the International Journal of Refrigeration, Butterworth & Co (Publishers) Ltd

The goal of this research was to determine evaporation and condensation heat transfer coefficients for HFC-134a. Measurements for CFC-12 were also taken to provide a base line for evaluating the relative performance of HFC-134a. A lack of published information on the heat transfer characteristics of HFC-134a prevented any comparisons with other experimental work. However, it was possible to compare the experimental results for HFC-134a with predicted heat transfer coefficients obtained from theoretical correlations.

Heat transfer coefficients for HFC-134a and CFC-12 were measured with an experimental rig capable of testing both single-phase and two-phase flow. This paper will review the main aspects of this experimental rig and the operational procedures used during testing. The main equations used in the data reduction are also reviewed. Results for single-phase, evaporation, and condensation of both HFC-134a and CFC-12 are given, and the performance of the two refrigerants are compared.

TEST FACILITIES

The test rig has three main parts: a refrigerant loop, a water loop, and a water-glycol loop. The refrigerant loop contains the test section, which consists of a horizontal smooth tube. The water loop contains the annulus that surrounds the test section and is used to heat or cool the refrigerant during testing. The water-glycol loop is used to subcool the refrigerant that leaves the test section. A schematic drawing of the test rig is shown in Figure 1.

Refrigerant loop

The refrigerant loop contains the test section, an after-condenser, a positive displacement pump, an accumulator bladder, a boiler, and a superheater. The test section is a horizontal smooth tube surrounded by an annulus. The inner tube in which the refrigerant flows is a 3.67-m-long smooth tube with an outer diameter of 9.25 mm and an inner diameter of 8.0 mm. The refrigerant is heated or cooled during testing by the water flowing in the outer annulus.

The after-condenser is a coaxial heat exchanger that subcools the refrigerant exiting the test section to $-15°C$. The subcooled refrigerant is then pumped with a positive displacement pump, which allows oil-free circulation in the refrigerant loop. The accumulator bladder sets the system pressure and dampens any fluctuations in the system. With the flow rate and pressure set, the quality entering the test section is controlled by using two heaters, namely a boiler and superheater, located just before the test section. The boiler is a 12.7-mm-o.d., 2.63-m-long stainless steel tube heated by direct electric current, while the superheater is a 12.7-mm-o.d., 1.83-m-long copper tube wrapped with a ceramic bead heater supplied with alternating current.

The refrigerant flow rate is measured by a positive displacement flow meter with an experimental uncertainty of $\pm 1\%$. The refrigerant pressure is measured at the inlet of the test section with a strain-gauge type pressure transducer, accurate to ± 9 kPa. The pressure drop of the refrigerant flowing through the test section is measured with a strain-gauge type differential pressure transducer accurate to ± 0.2kPa. A pair of thermocouples is located at the inlet and another pair at the exit of the test section.

Water loop

The water loop is used to supply water to the annulus side of the test section for the purpose of heating or cooling the refrigerant flowing in the test tube. The water loop consists of the test section annulus, a centrifugal pump, a magnetic flow meter, and a heat exchanger. The water flow rate is set by the centrifugal pump and a restricting valve. The temperature of the water in the line is controlled by the heat exchanger which can be supplied with warm or cold water from the building taps, depending on the temperature that is needed in the annulus. The magnetic flow meter measures the water flow rate with an experimental uncertainty of $\pm 2\%$. The temperature in the annulus is measured by two pairs of thermocouples, with one pair located at the inlet and the other pair at the exit of the annulus. From calibration of the thermocouples, an uncertainty of $\pm 0.2°C$ was found for the temperature difference measurements.

Water-glycol loop

The water-glycol loop contains a storage tank with a 209 L capacity, a centrifugal pump, a coaxial heat exchanger, and a 17.5 kW refrigeration unit. The refrigeration unit cools the fluid in the storage tank down to $-20\ C$. To keep this fluid from freezing, a 50/50 percent mixture of water and glycol is employed. This mixture is circulated by a centrifugal pump through the coaxial heat exchanger (in the refrigerant line), which is used to condense the refrigerant leaving the test section.

EXPERIMENTAL PROCEDURES

The system is allowed to come to steady state before final data aquisition is begun. Achieving steady state involves setting the refrigerant flow rate, annulus temperature difference, refrigerant pressure, and inlet and exit qualities of the refrigerant. A program in the controller checks for steady state by monitoring temperature changes in the system. When no changes in the temperature or flow rate can be detected, the final data acquisition program is initiated. This program runs for two minutes, scanning all channels a total of five times. Because of pressure fluctuations, the pressure drop channel is scanned a total of 35 times. The data for each channel are averaged and an arithmetic mean is calculated. If any large deviations due to unsteady effects are detected, the run is aborted.

DATA REDUCTION

The main equations used in the data reduction are based on energy balances performed on the test section assembly. The heat transferred in the test section is calculated from an energy balance on the water flowing in the annulus:

$$Q_{T_W} = M_W \cdot C_w \cdot (T_{W_{in}} - T_{W_{out}}) \tag{1}$$

During single-phase flow, the heat transferred in the test section can also be calculated from an energy balance on the refrigerant:

$$Q_{T_R} = M_R \cdot C_R \cdot (T_{R_{in}} - T_{R_{out}}) \tag{2}$$

A comparison of the water-side energy balance and the refrigerant-side energy balance provides a relative check of measurement accuracy. These two energy balances agreed to within 6% for all runs.

The refrigerant-side heat transfer coefficient can be determined from the overall heat transfer coefficient and the annulus-side heat transfer coefficient by using the procedures described below. The overall heat transfer coefficient is

$$U_o = \frac{Q_{T_W}}{A_o \cdot LMTD} \tag{3}$$

The log mean temperature difference is determined from the annulus-side inlet and exit temperatures and from the saturation temperatures at the inlet and exit of the test section:

$$LMTD = \frac{(\Delta T_1 - \Delta T_2)}{\ln(\Delta T_1 / \Delta T_2)} \tag{4}$$

where

$$\Delta T_1 = T_{sat_{out}} - T_{W_{in}} \tag{5}$$

$$\Delta T_2 = T_{sat_{in}} - T_{W_{out}} \tag{6}$$

The heat transfer coefficient of the water on the annulus side of the test section was calibrated by using a Wilson plot technique [1]. By assuming that the copper tube and fouling effects are negligible, the refrigerant heat transfer coefficient can be determined from

$$h_r = \frac{1}{\left(\frac{1}{U_o} - \frac{1}{h_w}\right)\frac{A_i}{A_o}} \quad (7)$$

This formula determines an average heat transfer coefficient over the length of the tube. The quality entering the test section is obtained from an energy balance on the preheaters, while the quality change in the test section is calculated from the energy balance on the water side.

Both single-phase flow and two-phase flow use equations (3) through (7) for calculating refrigerant-side heat transfer coefficients. However, if single-phase flow is present, then several adjustments are appropriate. Specifically, the LMTD of equation (4) is calculated from the thermocouple reading at the inlet and exit of the test section, and the Q_{T_w} of equation (3) is an average of the water-side and refrigerant-side energy balances.

A propagation-of-error method suggested by Kline and McClintock [2] was used to estimate the experimental uncertainty. During evaporation of HFC-134a, the experimental uncertainty in the heat transfer coefficient was $\pm 9\%$ at a mass flux of 400 $\frac{kg}{m^2 s}$ and $\pm 14\%$ at a mass flux of 130 $\frac{kg}{m^2 s}$. For condensation of HFC-134a, the experimental uncertainty in the heat transfer coefficient was $\pm 8\%$ at a mass flux of 400 $\frac{kg}{m^2 s}$ and $\pm 13\%$ at a mass flux of 130 $\frac{kg}{m^2 s}$. The experimental uncertainties in the heat transfer coefficients for CFC-12 were similar to those for HFC-134a. The experimental uncertainty in the refrigerant mass flux was $\pm 3\%$, while the quality had an experimental uncertainty of $\pm 3.5\%$.

TEST RESULTS

Experimental heat transfer coefficients are reported for HFC-134a and CFC-12 during single-phase flow, evaporation, and condensation. As mentioned earlier, the test tube was a 3.67-m-long smooth tube with an inner diameter of 8.0 mm. The range of test conditions was selected to reflect actual conditions in refrigeration systems. Because HFC-134a is a possible replacement for CFC-12, it is desirable to compare the refrigerants under the same operating conditions. The experimentally determined heat transfer coefficients are also used to determine which theoretical correlation best estimates the heat transfer coefficients for each refrigerant.

Single-phase

Single-phase heat transfer coefficients were determined at average temperatures ranging from 24 to 27°C and at mass fluxes ranging from 500 to 900 $\frac{kg}{m^2 s}$. Single-phase heat transfer tests were conducted because both evaporators and condensers operate with single-phase regions. Single-phase test are also used as a check on system accuracy because single-phase heat transfer correlations from the literature can accurately predict heat transfer coefficients.

Figure 2 presents the single-phase heat transfer coefficients for HFC-134a and CFC-12. The lines on the graph represent a least-squares fit of the plotted points for each refrigerant. For this series of tests, the refrigerant is being cooled. When the heat transfer coefficients for the two refrigerants are compared, HFC-134a shows a 30% increase over CFC-12. Most of the increase in heat transfer coefficients can be attributed to the increased liquid thermal conductivity of HFC-134a. For example, at 27°C the liquid thermal conductivity of HFC-134a is 81.4 $\frac{mW}{m\,K}$ [3] while for CFC-12 it is 69.7 $\frac{mW}{m\,K}$. This is a 17% increase in liquid thermal conductivity for HFC-134a.

The experimentally determined Nusselt numbers for HFC-134a and CFC-12 are compared with the Dittus-Boelter McAdams [4] and Petukhov-Popov [5] correlations. For HFC-134a the Petukhov-Popov correlation predicts the experimental Nusselt number within 2.5%, while the Dittus-Boelter predicts the Nusselt number within 24%. For CFC-12 the Petukhov-Popov correlation predicts the experimental Nusselt number within 1.5%, while the Dittus-Boelter correlation predicts Nusselt number within 25%. The Petukhov-Popov correlation has also been shown to be accurate for other refrigerants, such as HCFC-22 [1].

Evaporation

Evaporation tests were performed over a range of mass fluxes at three temperatures: 5°C, 10°C, and 15°C. Even though attempts were made to match the above temperatures, slight variations in evaporation temperature, ±1°, occurred between tests. The conditions for evaporation tests are summarized in Table 1. At the same mass flux, the heat flux was varied in order to obtain similar exiting qualities for the two refrigerants. This reflects the increased enthalpy of vaporization for HFC-134a. For example, at a mass flux of 200 $\frac{kg}{m^2 s}$ and a temperature of 10°C, the heat flux was 12.1 $\frac{kW}{m^2}$ for HFC-134a and 9.1 $\frac{kW}{m^2}$ for CFC-12.

Figure 3 shows evaporation heat transfer coefficient data versus mass flux for HFC-134a and CFC-12. The line representing each temperature is a least-squares fit of the data obtained at that temperature. Both HFC-134a and CFC-12 heat transfer coefficients increased with temperature and mass flux. Comparing the heat transfer coefficients for HFC-134a and CFC-12 at similar mass fluxes shows that HFC-134a has a 30 to 40% higher heat transfer coefficients than CFC-12. A more realistic comparison of the heat transfer coefficients for HFC-134a and CFC-12 at similar cooling capacities is discussed in a later section.

The above comparison is based on equivalent mass fluxes and quality change over a similar tube length. Therefore, the heat flux is higher for HFC-134a because the enthalpy of vaporization is greater for HFC-134a. An investigation of the effects of heat flux by using well-known correlations showed that the higher heat flux for HFC-134a compared to CFC-12 could increase the evaporation heat transfer coefficient by as much as 10%.

The experimental data were also compared to predictions from the correlations of Shah [6], Kandlikar [7], Chaddock-Brunemann [8], and Gungor-Winterton [9]. Local heat transfer coefficients from these correlations were numerically integrated over the whole quality range to obtain average heat transfer coefficients. For CFC-12, all correlations, except the Chaddock-Brunemann correlation, differ from experimental results by less than ±25%. The differences for the Shah correlation are even smaller, being less than ±15%. For HFC-134a, the predicted results for all correlations differ from experimental data by less than ±25%, with the Chaddock-Brunemann and Kandlikar correlation results differing from experimental results by less than ±15%. It should be noted that for HFC-134a, a fluid-dependent factor equivalent to the CFC-12 value, namely 1.5, was used in the Kandlikar correlation. However, the experimental data for HFC-134a was also used to determine the fluid-dependent factor in the Kandlikar correlation. Specifically, a fluid-dependent factor value of 1.63 was found to give the lowest deviation for all HFC-134a experimental data.

Condensation

Condensation tests were performed for a range of mass fluxes at three temperatures, 30°C, 40°C, and 50°C. As in the evaporation tests, variations of ±1° occurred at each temperature because of experimental limitations. The conditions for condensation tests are summarized in Table 2. As in the evaporation tests, the heat flux for HFC-134a was higher than that for CFC-12 because of the increased enthalpy of vaporization. However, it should be noted that at the mass fluxes tested in this study condensation heat transfer coefficients are not functions of heat flux.

Figure 4 presents condensation heat transfer coefficient data versus mass flux for HFC-134a and CFC-12. The lines are a least-squares fit of the data at each temperature. For both refrigerants, the heat transfer coefficients decrease with temperature but increase with mass flux. When the two refrigerants are compared to each other, HFC-134a results in 25 to 35% higher heat transfer coefficients. A more realistic comparison of the two refrigerants for condensation at similar heating capacities is presented in the next section.

The experimental heat transfer coefficients were compared with the Shah [10], Traviss et al. [11], and Cavallini-Zecchin [12] correlations. As in the evaporation case, these local heat transfer coefficients were integrated over the quality range to obtain average heat transfer coefficients. The differences between experimental and predicted heat transfer coefficients for CFC-12 are less than ±25% for all correlations. For condensation of HFC-134a, the differences between experimental and predicted heat transfer coefficients are less than ±25% for the Shah and the Cavallini-Zecchin correlations.

Comparison at equivalent cooling (heating) capacity

The experimental heat transfer coefficients for HFC-134a and CFC-12 are compared by forming the ratio of the heat transfer coefficients at similar cooling capacities. The cooling capacity comparison is based on approximating the cooling capacity of a system by multiplying the mass flow rate times the enthalpy of vaporization. For the condensation case, the value obtained is actually an equivalent heating capacity. It should also be noted that this comparison is base on using the same tube diameters for both HFC-134a and CFC-12 applications.

Figure 5 compares heat transfer coefficients for HFC-134a and CFC-12 at an equivalent cooling (and heating) capacity for evaporation (and condensation). The equivalent cooling capacity ratio is formed from the least-squares fit of the evaporation heat transfer coefficients plotted in Figure 3, while the equivalent heating capacity for condensation is formed from the condensation heat transfer coefficients plotted in Figure 4. Specifically, these capacity ratios are formed from heat transfer coefficients taken at equivalent values of mass flow rate times the enthalpy of vaporization of the refrigerant. Because the enthalpy of vaporization is higher for HFC-134a, the heat transfer coefficient ratio is formed with the HFC-134a flow rate being significantly reduced compared to CFC-12. Even with the reduced flow rate, the HFC-134a-to-CFC-12 ratio for equivalent cooling capacities is still 1.05 to 1.15, while the HFC-134a-to-CFC-12 ratio for equivalent heating capacities is 1.10 to 1.20.

CONCLUSIONS

Heat transfer coefficients were experimentally determined for HFC-134a and CFC-12. In single-phase flow, heat transfer coefficients for HFC-134a were 33% higher when compared to those of CFC-12. For evaporation at similar mass fluxes, HFC-134a heat transfer coefficients were 35 to 45% higher than those of CFC-12. For condensation at similar mass fluxes, HFC-134a heat transfer coefficients were 25 to 35% higher than those of CFC-12. The heat transfer coefficients for the two refrigerants were also compared at different flow which produce equivalent cooling and heating capacities. Equivalent cooling and heating capacities were approximated by multiplying mass flow rate and enthalpies of vaporization. Because the enthalpy of vaporization is higher for HFC-134a, the heat transfer coefficient comparison is made with the HFC-134a flow rate being significantly reduced compared to CFC-12. For this situation, HFC-134a resulted in 5 to 15% higher heat transfer coefficients. When the two refrigerants are compared for equivalent heating capacity in a condenser, HFC-134a resulted in heat transfer coefficients that were 10 to 20% higher.

ACKNOWLEDGMENTS

The authors would like to thank E. I. Du Pont De Nemours & Company (Inc.) for sponsoring this project and for supplying the HFC-134a. The authors would also like to extend a special thanks to Dr. Don Bivens of Du Pont for his support and helpful suggestions.

REFERENCES

1. **Schlager, L. M., Pate, M. B., Bergles, A. E.** Evaporation and condensation of refrigerant-oil mixtures in a smooth tube and micro-fin tube *ASHRAE Transactions* (1988) **93**(1) 293-416

2. **Kline, S. J., McClintock, F. A.** Describing uncertainties in simple sample experiments *Mechanical Engineering* (1953) **75** 3-8

3. **Bivens, D. B.** E.I. Du Pont De Nemours & Company, Inc. *private communications* (1989)

4. **McAdams, W. H.** *Heat Transmission* 2nd ed. McGraw-Hill, New York, USA (1942)

5. **Petukhov, B. S.** Heat transfer and friction in turbulent pipe flow with variable physical properties *Advances in Heat Transfer* Vol 6 Academic Press, New York, USA (1970) 503-564

6 **Shah, M. M.** Chart correlation for saturated boiling heat transfer: equations and further study *ASHRAE Transactions* (1982) **88**(1) 66-86

7 **Kandlikar, S. S.** A general correlation for saturated two-phase flow and boiling heat transfer inside horizontal and vertical tubes *Boiling and Condensation in Heat Transfer Equipment* ASME, New York, USA (1987) **85** 9-19

8 **Chaddock, J. B., Brunemann, H.** Forced convection boiling of refrigerants in horizontal tubes-Phase 3, HL-113, Duke University School of Engineering, Durham, N.C., USA (1967)

9 **Gungor, K. E., Winterton, R. H. S.** A general correlation for flow boiling tubes and annuli *International Journal of Heat and Mass Transfer* (1986) **29** 351-58

10 **Shah, M. M.** A general correlation for heat transfer during film condensation inside pipes *International Journal of Heat and Mass Transfer* (1979) **88** 185-196

11 **Traviss, D. P., Rohsenow, W. M., Baron, A. B.** Forced convection condensation inside tubes: A heat transfer equation for condenser design *ASHRAE Transactions* (1972) **79**(1) 157-65

12 **Cavallini, A., Zecchin, R.** A dimensionless correlation for heat transfer in forced convection condensation In Vol.III *Proceedings of the Fifth International Heat Transfer Tokyo* (1974) **3** 309-313

Table 1: Evaporation test conditions

hline	CFC-12	HFC-134a
Temperature	$5 - 15°C$	$5 - 15°C$
Pressure	0.36-0.49 MPa	0.35-0.49 MPa
Mass flux	125-400 $\frac{kg}{m^2 s}$	125-400 $\frac{kg}{m^2 s}$
Quality in	5-10%	5-15%
Quality out	80-88%	80-88 %

Table 2: Condensation test conditions

	CFC-12	HFC-134a
Temperature	$30 - 50°C$	$30 - 50°C$
Pressure	0.75-1.24 MPa	0.76-1.32 MPa
Mass flux	125-400 $\frac{kg}{m^2 s}$	125-400 $\frac{kg}{m^2 s}$
Quality in	80-88%	80-88%
Quality out	8-15%	10-20%

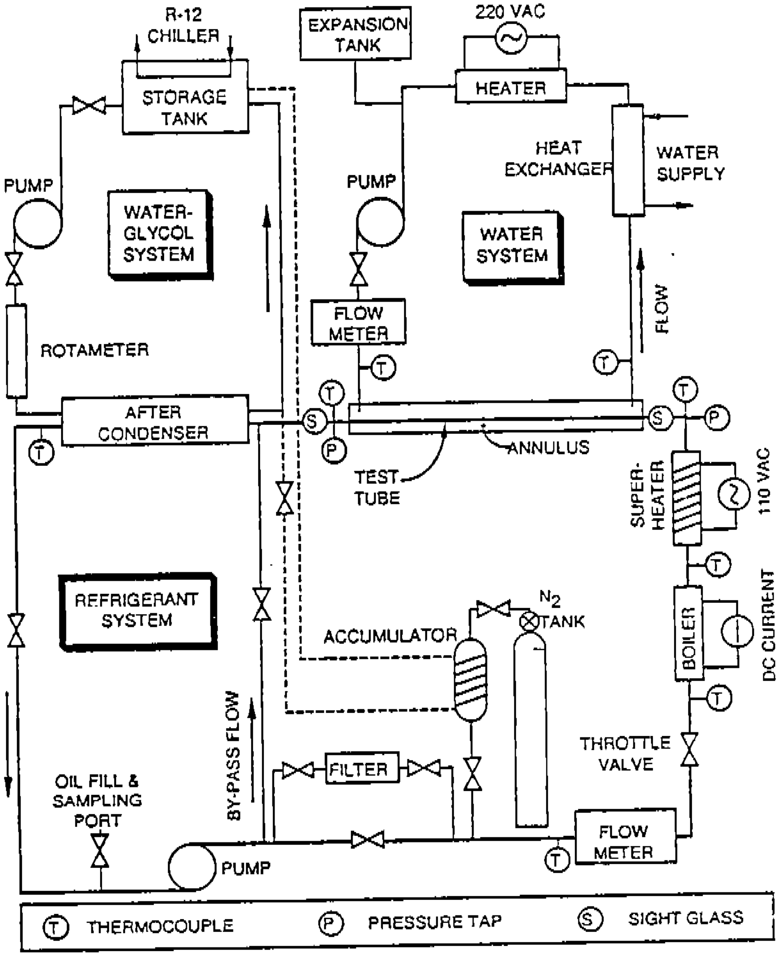

Figure 1: Schematic drawing of test facilities

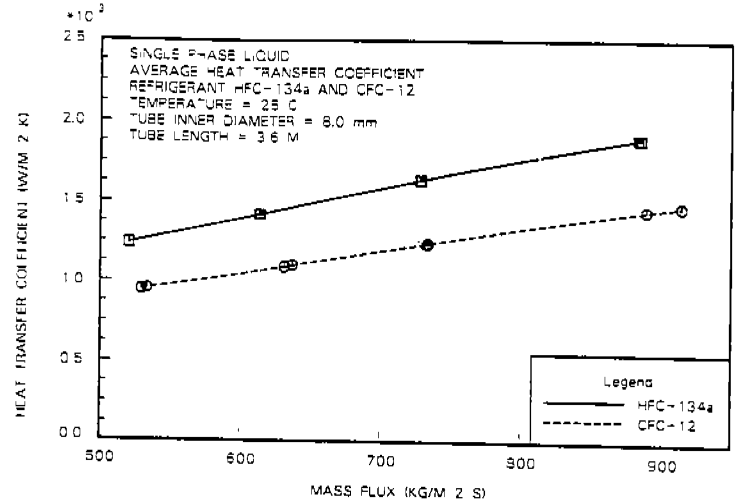

Figure 2: Measured single-phase heat transfer coefficients for HFC-134a and CFC-12

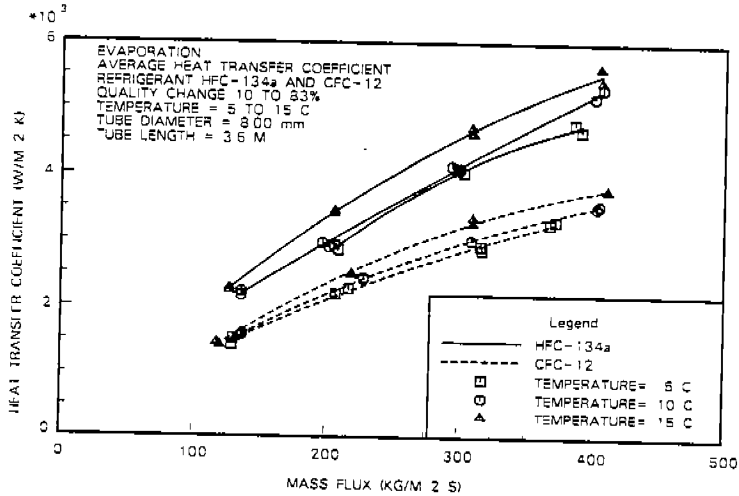

Figure 3: Measured evaporation heat transfer coefficients for HFC-134a and CFC-12 at three temperatures

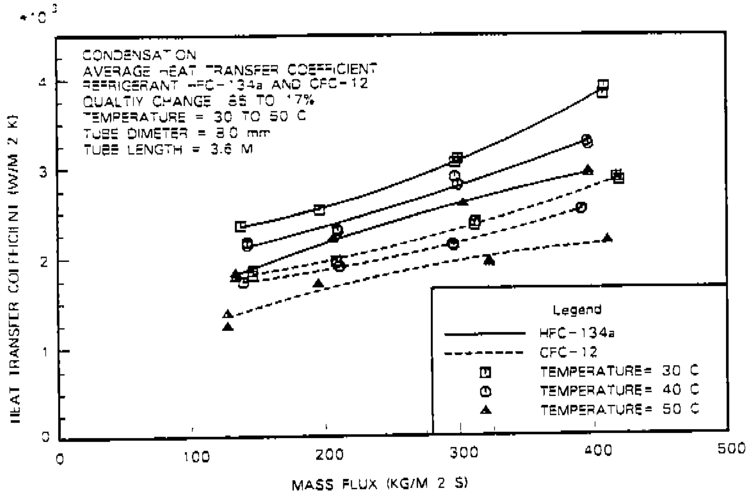

Figure 4: Measured condensation heat transfer coefficients for HFC-134a and CFC-12 at three temperatures.

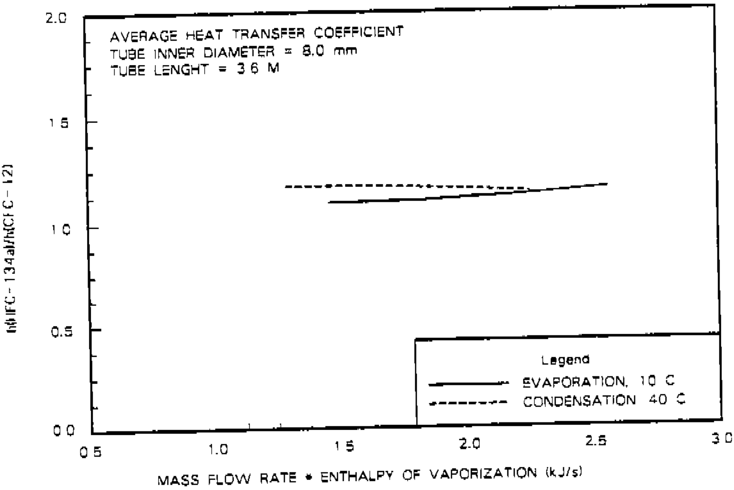

Figure 5: Ratio of HFC-134a-to-CFC-12 measured heat transfer coefficients for similar cooling and heating capacities